



## Article (refereed) – Published version

---

Prieto, E.; González-Pola, C.; Lavín, A.; **Holliday, N.P.**. 2015 Interannual variability of the northwestern Iberia deep ocean: Response to large-scale North Atlantic forcing. *Journal of Geophysical Research: Oceans*, 120 (2). [10.1002/2014JC010436](https://doi.org/10.1002/2014JC010436)

This version available at <http://nora.nerc.ac.uk/509714/>

NERC has developed NORA to enable users to access research outputs wholly or partially funded by NERC. Copyright and other rights for material on this site are retained by the rights owners. Users should read the terms and conditions of use of this material at

<http://nora.nerc.ac.uk/policies.html#access>

**AGU Publisher statement: An edited version of this paper was published by AGU. Copyright (2015) American Geophysical Union. Further reproduction or electronic distribution is not permitted.**

Prieto, E.; González-Pola, C.; Lavín, A.; **Holliday, N.P.**. 2015 Interannual variability of the northwestern Iberia deep ocean: Response to large-scale North Atlantic forcing. *Journal of Geophysical Research: Oceans*, 120 (2). [10.1002/2014JC010436](https://doi.org/10.1002/2014JC010436)

To view the published open abstract, go to <http://dx.doi.org/10.1002/2014JC010436>

Contact NOC NORA team at  
[publications@noc.soton.ac.uk](mailto:publications@noc.soton.ac.uk)

## RESEARCH ARTICLE

10.1002/2014JC010436

## Interannual variability of the northwestern Iberia deep ocean: Response to large-scale North Atlantic forcing

E. Prieto<sup>1</sup>, C. González-Pola<sup>1</sup>, A. Lavín<sup>2</sup>, and N. P. Holliday<sup>3</sup><sup>1</sup>Instituto Español de Oceanografía, Centro Oceanográfico de Gijón, Gijón, Spain, <sup>2</sup>Instituto Español de Oceanografía, Centro Oceanográfico de Santander, Santander, Spain, <sup>3</sup>National Oceanography Centre, Southampton, UK

## Key Points:

- The 2003–2013 hydrographical variability of the NW Iberia deep ocean is analyzed
- Background slow-varying signals dominate over short-term variability
- Property shifts across most water column follow extreme states of winter NAO

## Correspondence to:

E. Prieto,  
epb.ocean@gmail.com

## Citation:

Prieto, E., C. González-Pola, A. Lavín, and N. P. Holliday (2015), Interannual variability of the northwestern Iberia deep ocean: Response to large-scale North Atlantic forcing, *J. Geophys. Res. Oceans*, 120, 832–847, doi:10.1002/2014JC010436.

Received 30 SEP 2014

Accepted 13 JAN 2015

Accepted article online 21 JAN 2015

Published online 12 FEB 2015

**Abstract** The oceanic hydrography of the north-easternmost region of the North Atlantic subtropical gyre has been monitored since 2003 by three sections extending between 100 and 200 nautical miles from the Spanish NW and N coast into the Atlantic and the Bay of Biscay. The sections were occupied twice a year from 2003 to 2010, annually after that, and measure the whole water column (>5000 m). Correlation of series in the vertical and among sections, autocorrelation and estimates of the effect of the noise induced by the mesoscale field, all indicate that observed signatures are robust changes of water masses at the regional scale. The hydrographic time series are not characterized by smooth trends but instead by shifts that persist through consecutive cruises. The most notable features include a shift to more saline central waters around 2005 after which they remained stable, and a decrease in thermohaline properties of the Labrador Sea Water from autumn 2008 to 2010. Years with a strong winter North Atlantic Oscillation (NAO) index are characterized by shifts in thermohaline properties across most of the intermediate levels, with the most notable event being the warming and increasing salinity that followed the large NAO index drop of 2010. The observations are consistent with current understanding of the large-scale functioning of the North Atlantic, which predicts a northeastward expansion of subtropical temperate waters in the eastern boundary as a response to NAO forcing. The observed variability is discussed in relationship to large-scale circulation.

## 1. Introduction

The ocean is assumed to be absorbing large amounts of heat in response to ongoing climate change [Barnett *et al.*, 2005], but due to the nonlinear responses of complex ocean-atmosphere system, this does not imply sustained long-term trends in hydrographic properties at all basins or sites but rather a more heterogeneous response. Moreover, the different time scales of variability require sufficiently long and regularly sampled time series to detect long-term trends [Wunsch, 1999]. Oscillations on decadal time scales appear naturally in the climate system [Latif and Barnett, 1996] and so caution is needed when treating any observed change in water mass properties or ocean circulation as an indicator of climate change [e.g., Bryden *et al.*, 2003]. For these reasons, the establishment of systematic and sustained programs of ocean observation is a recurrent request from scientists and oceanographic governance and coordination panels as ICES, CIESM, GOOS, or GLOBEC [e.g., Dexter and Summerhayes, 2002; Baker *et al.*, 2007; Hughes *et al.*, 2012; Lindstrom *et al.*, 2012].

The North Atlantic, a key area for the global climate system due to the presence of the Atlantic Meridional Overturning Circulation (AMOC), is subject to strong interannual, decadal, and multidecadal variability. In particular, hydrographic sections in the subpolar gyre from the coast of the Labrador Sea to Europe show a multidecadal variability in temperature, while convective events occur on decadal or shorter time scales [van Aken *et al.*, 2011]. Such events were shown to homogenize the properties of intermediate layers for significant periods of time, emphasizing the leading role of Labrador Sea convection as a driving mechanism of the variability of intermediate water layers in the North Atlantic. Recent warming over the upper 3000 m of the North Atlantic has been attributed to both long-term climate change (including anthropogenic) and natural multidecadal variability, the latter accounting up to a 60% of the warming since 1970 [Polyakov *et al.*, 2010]. Embedded in this positive phase of multidecadal variability characterized by warmer than normal conditions both in the land and sea, 2000–2010 was the warmest decade on record, reaching the highest global average temperatures in 2010 [Hansen *et al.*, 2010]. Changes in the subpolar North Atlantic

hydrographic properties are tightly related to large-scale atmospheric forcing induced by the North Atlantic Oscillation, NAO [e.g., *Sarafanov*, 2009]; however, an overall weak and variable NAO during the first decade of the present century made the relationship less robust [*Hughes et al.*, 2012]. The North Atlantic Subpolar Gyre (SPG) index was recently proposed as a further indicator of ocean variability that should be considered in climate change studies [*Häkkinen and Rhines*, 2004; *Hätún et al.*, 2005]. Interpretation of the SPG index invokes wind stress curl as a possible forcing mechanism for changes in the pathways of subtropical waters, and the subsequent effect on temperature and salinity of the subpolar region [*Häkkinen and Rhines*, 2009].

There are a number of well-established monitoring programs in the subpolar regions that have led to long time series [*Sarafanov et al.*, 2010; *Hughes et al.*, 2012], and the subtropical Atlantic has been sampled by the repetition of the WOCE A5 26.5°N transatlantic section on regular basis since 2004 [*Cunningham et al.*, 2007]. However the temperate midlatitude areas have been observed less frequently. We use 11 year time series of oceanographic sections in that part of the midlatitude North Atlantic eastern boundary located off the northwestern Iberia and southern Bay of Biscay, to describe the interannual thermohaline changes observed during 2003–2013. We relate local regional changes with changes observed in other distant regions and interpret the outcomes in the context of main driving mechanisms of North Atlantic Ocean variability. The regional oceanography and water masses are briefly presented in section 2. The data set used in this study is presented in section 3, and section 4 shows the methodology applied for the treatment of the hydrographic record. The results are shown in section 5 and discussed in section 6 in terms of the main driving mechanisms of North Atlantic variability at different time scales. Finally, the main conclusions of the work are summarized in section 7.

## 2. Regional Oceanography and Water Masses of the North-West Iberia Peninsula

Our study region, the western Iberian margin, is located at the north-easternmost part of the subtropical gyre (North Atlantic eastern boundary), sometimes referred to as the intergyre region (Figures 1a and 1b). This region is characterized by a weak upper ocean circulation with a mean southward flow of few  $\text{cm s}^{-1}$  [*Mazé et al.*, 1997; *Paillet and Mercier*, 1997], affected by an important mesoscale activity [*Memery et al.*, 2005].

Bathymetry in the region is characterized by a narrow continental shelf ( $\sim 25$  km) and a steep continental slope associated with the development of a density-driven poleward current known as the Iberian Poleward Current (IPC) [e.g., *Frouin et al.*, 1990; *Peliz et al.*, 2005]. A detailed review of the modal, intermediate, and deep water masses of the midlatitude northeast Atlantic Ocean was performed by *van Aken* [2000a, 2000b, 2001]. *Prieto et al.* [2013] provide a more specific description of the local water masses and circulation patterns for a study of seasonality based on the same data set described here. The pathways of water masses from their source regions toward western Iberia are sketched in Figure 1a and their positions in the potential temperature versus salinity diagram ( $\theta$ - $S$ ) are shown in Figure 1c. Briefly, these are as follows: the upper permanent thermocline of the European and northwest African basins is formed by the Eastern North Atlantic Central Water (ENACW, 200–400 dbar, core  $\sim 350$  dbar), ventilated yearly by winter mixing in a wide region from the Azores to the European boundary bounded by the North Atlantic Current (NAC) and the Azores Current (AC) [*Pollard and Pu*, 1985; *Pollard et al.*, 1996]. The lower bound of ENACW is characterized by the Salinity Minimum (400–600 dbar) centered at  $\sim 500$  dbar and separating the relatively fresh water of the upper thermocline from the salty Mediterranean Water (MW, 800–1200 dbar), a water formed at the exit of the Strait of Gibraltar in the Gulf of Cádiz from the intense mixing of Atlantic central waters and the warm, salty overflow from the Mediterranean Sea. The core of MW ( $\sim 1000$  dbar) is characterized by a marked salinity maximum flowing as a northward deep boundary current along the European ocean margin [*Iorga and Lozier*, 1999]. Below, a deep salinity minimum appears associated with the Labrador Sea Water (LSW), a water formed by winter convection in the Labrador Sea. The core of this water mass lies at  $\sim 1900$  dbar in the midlatitude Northeast Atlantic Ocean [*Pingree*, 1973; *van Aken*, 2000b]. Below LSW lies the Eastern North Atlantic Deep Water (ENADW, 2000–4000 dbar), and the Lower Deep Water (LDW) which is bottom water deeper than 4000 dbar [*van Aken*, 2000a].

## 3. Data Set: the VACLAN/COVACLAN Projects

A monitoring program of ocean properties has been in place since 2003 in the southern Bay of Biscay and northwestern Iberia margin, under the VACLAN/COVACLAN projects (Spanish acronym of “Coordination

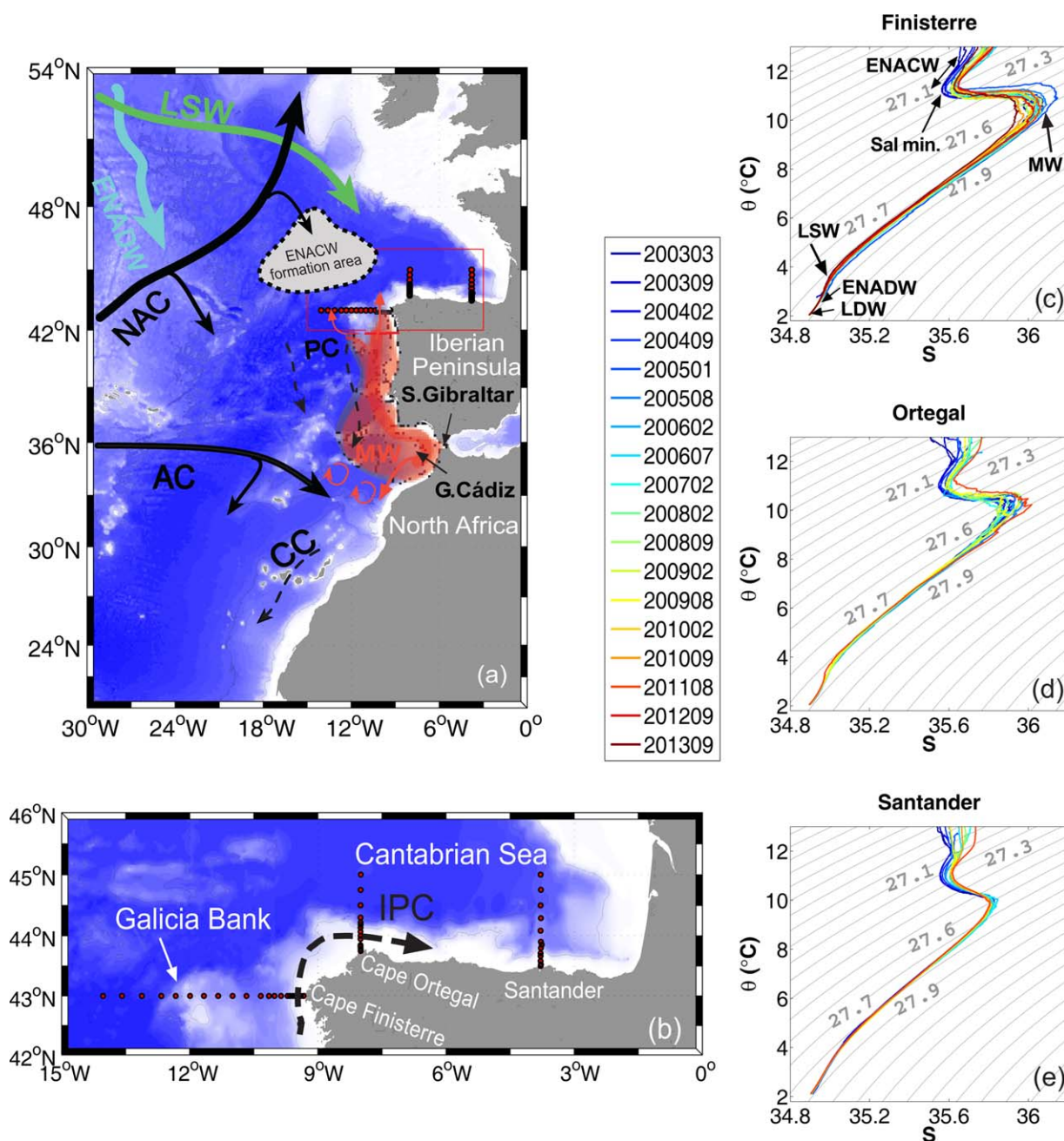


**Figure 1.** (a) Main circulation patterns of waters in the area. Gyres bounding North Atlantic Current (NAC) and Azores Current (AC) (black bold), southward flowing Portugal Current (PC) and Canary Current (CC) (black dashed). Central water: ENACW formation area is shown as a dashed gray region north of Finisterre, from where it flows southward with the PC. Intermediate waters: Mediterranean water (MW, red), spreading from the Strait of Gibraltar, flows northward along the continental slope sometimes showing a detachment contouring the west Galicia Bank, and southward flowing water from the Labrador Sea (LSW, green). Eastern North Atlantic Deep Water (ENADW, blue). Lower Deep Water (LDW). (b) Map of the VACLAN/COVACLAN sampling region including the Finisterre (western Iberia margin), Ortegal (southwestern Bay of Biscay), and Santander (southeastern Bay of Biscay) sections. Iberian Poleward Current (IPC) path is also shown. (c–e) From top to bottom,  $\theta/S$  diagram of along-section profile averages in Finisterre, Ortegal, and Santander, between 2003 (darkest blue) and 2013 (darkest red).

and optimization of the Northeast Atlantic Climate Variability Observing System”) of the Spanish Institute of Oceanography. The program aims to maintain a continuous observation program of climate variability in this region of the North Atlantic eastern boundary (see Figure 1b). Three deep sections perpendicular to the coast extend to 200 nm off Cape Finisterre (northwestern Iberia, 43°N, > 5000 m), 100 nm off Cape Ortegal (southwestern Bay of Biscay, 8°W, ~5000 m), and 100 nm off Santander (southeastern Bay of Biscay, 3°47’W, ~4000 m). The sections were sampled twice a year from 2003 to 2010 (except 2007) around winter

**Table 1.** VACLAN/COVACLAN Series of Cruises<sup>a</sup>

Cruise	Dates	N <sub>Fist.</sub>	N <sub>Orte.</sub>	N <sub>Sant.</sub>
RadProf200303	26 Mar 2003 to 17 Apr 2003	13	11	11
RadProf200309	10–20 Sep 2003	16	8	11
RadProf200402	5–13 Feb 2004	18	11	12
RadProf200409	7–13 Sep 2004	18	11	11
RadProf200501	27 Jan 2005 to 3 Feb 2005	6	10	9
RadProf200508	20 Aug 2005 to 9 Sep 2005	20	14	12
RadProf200602	5–13 Feb 2006	19	14	12
RadProf200607	12–29 Jul 2006	19	13	10
RadProf200702	1–7 Feb 2007	21	14	6
RadProf200802	11–19 Feb 2008	19	14	12
RadProf200809	3–13 Sep 2008	18	14	12
RadProf200902	1–13 Feb 2009	15	13	10
RadProf200908	11–21 Aug 2009	19	14	12
RadProf201002	9–11 Feb 2010	19		
RadProf201009	2–11 Sep 2010	19		12
RadProf201108	14–24 Aug 2011	21	14	12
RadProf201209	12–16 Sep 2012	23		
RadProf201309	13–17 Sep 2013	24		

<sup>a</sup>“RadProf” is an acronym for the Spanish of “Deep Section.” Dates and number of stations sampled at Finisterre (N<sub>Fist.</sub>, 43°N), Ortegale (N<sub>Orte.</sub>, 8°W), and Santander (N<sub>Sant.</sub>, 3°47'W).

and summer (within January–April and July–September), with data collected to WOCE standards [Joyce *et al.*, 1994]. In 2011, sections were only sampled in summer, and only sampling along the Finisterre section was performed in summer 2012 and 2013. The number of sampled stations and the start/end dates of surveys are shown in Table 1, where N<sub>Fist.</sub>, N<sub>Orte.</sub>, and N<sub>Sant.</sub> refer to the number of stations sampled at Finisterre, Ortegale, and Santander sections, respectively. Note that the Finisterre section was occupied a total of 18 times during the sampling period, becoming the most repeated, the longest, and the deepest sampled transect. Ortegale section was not sampled, besides 2012–2013, in February or

September 2010 (14 occupations), and Santander section was not sampled in February 2010 (15 occupations). Table 2 summarizes properties of water masses separated by density layers (following the scheme devised by van Aken [2000a, 2000b, 2001]) with corresponding along-section mean values of pressure, potential temperature, and practical salinity. The diagrams of Figures 1c–1e provide a first overview of the year-to-year thermohaline variability in all depths of the water column.

#### 4. Methods

In order to quantify interannual changes in water properties, it is necessary to extract the seasonal cycle. The Finisterre series showed seasonality of the deep ocean down to 2000 dbar [Prieto *et al.*, 2013], mostly evidenced as a MW vein detaching from the slope and spreading out to the open ocean in wintertime. Seasonality accounts for up to 20% of interannual variations observed in the thermohaline properties of our 43°N section. The deseasonalized signal is computed by subtracting each cruise section from the corresponding winter (summer) average field, i.e.,

$$\theta_i^{\text{des}} = \theta_i - \bar{\theta}_{\text{winter/summer}}, \quad S_i^{\text{des}} = S_i - \bar{S}_{\text{winter/summer}} \quad (1)$$

where *i* is the number of repeats of a section and superscript “des” refers to the deseasonalized field. Anomalies are calculated at each profile site and then zonally averaged for every cruise *i*. Next, the anomalies are vertically averaged within pressure intervals 0–200, 200–400, and from 400 dbar to the bottom. Finally, changes of properties along pressure surfaces are decomposed into changes along isopycnals (isopycnal change) plus changes due to the displacement of isopycnals (heave) following the work of Bindoff and McDougall [1994]. Neutral density  $\gamma^n$  [Jackett and McDougall, 1997] is normally taken as the density

**Table 2.** Potential Density Layers Defining Water Masses According to van Aken [2000a, 2000b, 2001]<sup>a</sup>

Water Mass	Density (kg m <sup>-3</sup> )	$\gamma^n$ (kg m <sup>-3</sup> )	$\bar{P}_{\text{Fist.}}$	$\bar{\theta}_{\text{Fist.}}$	$\bar{S}_{\text{Fist.}}$	$\bar{P}_{\text{Orte.}}$	$\bar{\theta}_{\text{Orte.}}$	$\bar{S}_{\text{Orte.}}$	$\bar{P}_{\text{Sant.}}$	$\bar{\theta}_{\text{Sant.}}$	$\bar{S}_{\text{Sant.}}$
ENACW	27.00 < $\sigma_\theta$ < 27.20	27.06–27.26	297	12.16	35.70	278	11.92	35.64	265	11.84	35.61
Sal min	$\sigma_\theta \approx 27.2$	27.26	475	11.30	35.61	463	11.22	35.59	457	11.22	35.59
MW	31.85 < $\sigma_1$ < 32.25	27.46–27.79	1002	10.07	35.85	1033	9.41	35.69	1020	9.18	35.63
LSW (core)	$\sigma_2 \approx 36.88$	27.93	1764	4.64	35.13	1786	4.41	35.08	1778	4.57	35.12
ENADW	41.42 < $\sigma_3$ < 41.51	28.02–28.10	3236	2.60	34.94	3230	2.59	34.94	3226	2.59	34.94
LDW (core)	$\sigma_4 \approx 45.83$	28.09	4500	2.08	34.90	4500	2.09	34.90	>4000	2.12	34.90

<sup>a</sup>Corresponding neutral densities ( $\gamma^n$ ) [Jackett and McDougall, 1997] and depth-averaged values of pressure ( $\bar{P}$ ), potential temperature ( $\bar{\theta}$ ), and salinity ( $\bar{S}$ ) along Finisterre (subscript *Fist.*), Ortegale (*Orte.*), and Santander (*Sant.*).

reference variable since it improves the behavior of potential density in layers of weak stability. We will use neutral surfaces along the paper although we may refer indistinctly to isopycnal or isoneutral levels.

Mathematically, the decomposition is as follows

$$\left. \frac{d\theta}{dt} \right|_p = \left. \frac{d\theta}{dt} \right|_n - \left. \frac{dp}{dt} \right|_n \frac{\partial \theta}{\partial p} \quad (2)$$

$$\left. \frac{dS}{dt} \right|_p = \left. \frac{dS}{dt} \right|_n - \left. \frac{dp}{dt} \right|_n \frac{\partial S}{\partial p} \quad (3)$$

where  $t$  indicates time and  $p$  and  $n$  indicate derivatives at pressure or neutral density levels, respectively. The approach assumes that vertical gradients of properties are constant over time. The left-hand term is known as the isobaric change, the first right-hand term the isopycnal change, and the second one the heave term. The isopycnal change accounts for density-preserving variations in the thermohaline properties of water masses (i.e., leaving an imprint in the  $\theta/S$  diagram). This term is normally related to intrinsic changes of water masses at the formation sites, thus is dependent on heat and freshwater fluxes in the source region. On the other hand, the heave term reflects the deepening or shoaling of associated isoneutrals (i.e., levels of constant neutral density) and can be related to changes in circulation or in the renewal rates of water masses. We will apply the methodology for the decomposition of changes using neutral density surfaces every  $0.1 \text{ kg m}^{-3}$ , in the water column between  $27$  and  $28 \text{ kg m}^{-3}$ .

An important issue is the magnitude of the high frequency variability along the section. We expect that our series are representative of the slow-varying changes in water masses properties at a regional scale. Without a higher sampling rate of the section, it is not possible to quantify the bias induced by mesoscale and/or short-term shifts in circulation fields, but some complementary approaches may be considered. First, if the slow-varying background properties dominate over the short-term mesoscale-induced changes, the series should exhibit autocorrelation. Second, if the series are representative of the regional background hydrographical variability there should be correlation (synchronous variation) between the three different sections at the same levels and across large portions of the water column. Finally, an external estimate of the uncertainty caused by the sampling rate can be evaluated by taking a low-passed version of a higher-frequency float-based product. The procedure will be explained in detail in section 5.2.

## 5. Results

### 5.1. Raw Time Series at Isobaric Levels: Overall Trends

A first insight of the evolution of thermohaline properties of water masses with time is provided by the  $\theta S$  diagrams in Figures 1c–1e. Note the isopycnal shift of central waters toward a warmer/more saline type at all three sections, seen here as the displacement of the straight line between 27.1 and 27.3 in the  $\theta S$  diagram. At deeper water below about  $\sigma_\theta \sim 27.4$ , the diagrams show no clear changes in properties. Figure 2 shows average temperature and salinity time series at isobaric levels in order to emphasize interannual changes at the three sections. Linear trends with confidence intervals derived from a  $t$  test at all layers are shown in Figure 3.

There is some coherent pattern in changes between the sections and through the water column, as well as notable year-to-year changes. Changes in the upper layer (surface to the maximum development of winter mixed layers, 200 dbar) are not well sampled by semiannual sections but the imprint of the cold winters 2005, 2006, and 2009 clearly emerges as described below. The surface salinity is characterized by two periods of smooth increase either side of the cold, fresh winter of 2009. The upper ENACW (200–400 dbar) shows a salinity rise of about 0.5 during 2005 and 2006 and remained pretty stable since then, yielding an overall salt-increase trend of  $0.006 \text{ year}^{-1}$ . A  $0.30^\circ\text{C}$  decrease in potential temperature in the 200–400 dbar layer at Finisterre indicates that the strong cooling in winter 2005 was able to penetrate deep in the water column. The effect was transitory since this layer and 400–800 dbar (the Salinity Minimum at the base of ENACW to the upper MW) show a significant warming trend of  $0.018\text{--}0.016^\circ\text{C yr}^{-1}$  over the time series. Lower thermocline waters (27.5–27.9, 800–2000 dbar including MW and LSW) are characterized by a drop in temperature and salinity in late 2008 and a recovery in 2011. The 1200–1600 dbar layer is the only part of the water column with overall significant negative trends in thermohaline properties. The deep water (28–

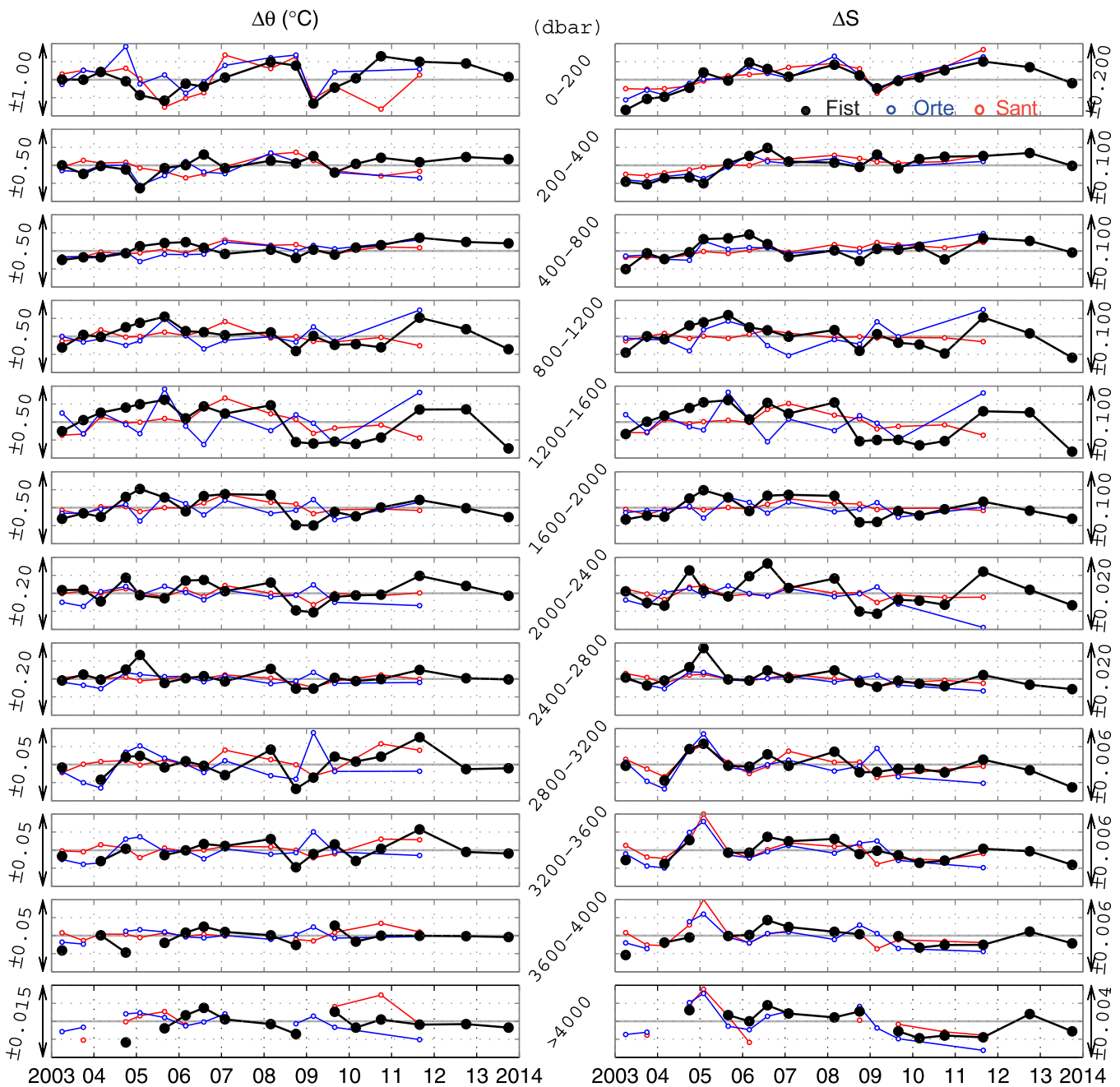


**Figure 2.** Potential temperature (left) and salinity (right) interannual variability, as anomaly from the mean seasonal value, at Finisterre (black), Ortegal (blue), and Santander (red) during 2003–2013. Changes were averaged over pressure intervals from surface to 200 dbar and then every 400 dbar down to 4000 dbar. Abyssal water (>4000 dbar) changes were averaged from 4000 dbar to the bottom.

28.1, ~2000 dbar to >4000 dbar) showed much weaker interannual variations. A freshening of >3600 dbar water (including bottom water) of about 0.004 was observed along the three transects from late 2009 to late 2012. There was coherent variation across most of the water column in 2008 and 2013 (cooling and decreasing salinity) and 2011 (warming and increasing salinity). Next, we examine the robustness of the signals described above by considering the effect of the sampling frequency on the results.

**5.2. Consistency of the Record: Correlation, Autocorrelation, and Mesoscale Field**

A well-acknowledged problem when describing the state and the evolution of ocean hydrography from repeated hydrographic sections is to identify the uncertainty induced by the mesoscale

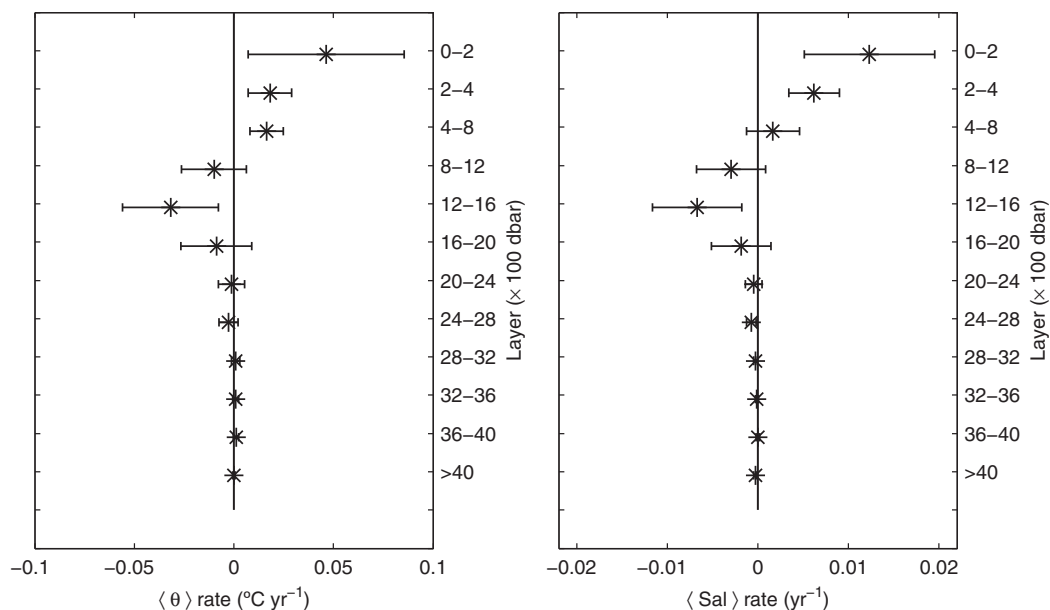


**Figure 3.** Potential (left) temperature and (right) salinity linear trends for series at Finisterre during 2003–2013 as shown in Figure 2.

variability in the region exhibit length scales of about 50–100 km diameter and decay scales of  $\sim 250 \pm 100$  days [Pingree, 1994] that may be a source of noise for our semiannual time series. Mesoscale structures are mostly originated at the slope [Pingree and Le Cann, 1992a, 1992b] and MW levels [Richardson et al., 2000]. Eddy-like structures are evident in the sections (not shown) and, accordingly, an estimate of correlation scale by a bestfit of salinity fields through an isotropic Gaussian function of the distance between the observations [e.g., Bretherton et al., 1976] yielded a decay scale of  $\sim 10$ –30 km. Average station spacing is about 25 km (closer in the shelf-break and increasing to 37 km at the outer ocean) so the mesoscale field should be captured by the sampling scheme. In this section, we use a statistical approach to infer which parts of the water column may be dominated by mesoscale variability.

If the short-term variability induced by the mesoscale field was greater than or comparable to the large-scale interannual variability, we would expect the series to be no different to noise and have no autocorrelation. To detect the presence of autocorrelation in the record (that is, to test the existence of statistically significant temporal coherence of variability), we applied a Durbin-Watson test [e.g., von Storch and Zwiers, 2001] to the series on isobars (Figure 2). Table 3 show the  $p$ -values; most surface to 2000 dbar Finisterre and Santander series indicate autocorrelation ( $p$ -values below 0.10 or 0.05 for most series), which suggests that series are dominated by the large-scale background signal. The Ortegale series fail the autocorrelation tests indicating that these series are more strongly affected by local short-term circulation and the mesoscale field. Deeper layers, below 2000 m, do not show autocorrelation in any of the sections. As no relevant trends or shifts of hydrographical properties have occurred at great depths, the lack of autocorrelation only indicates that weak variability of these stable water masses occurs at temporal scales shorter than the semiannual sampling.

If the mesoscale field was dominant in a section, we would expect that properties would only correlate vertically at the scale of eddies (within a single 400 dbar layer or two contiguous layers at most). In contrast, if changes were caused by shifts in large-scale advective patterns, there may be correlation across a greater pressure range. Correlation coefficients ( $R$ ) with associated  $p$ -values ( $p$ ) were calculated to test the hypothesis that there is no correlation between the isobaric levels shown in Figure 2. Table 4 shows correlation coefficients and  $p$ -values for potential temperature and salinity anomalies along the Finisterre, Ortegale, and Santander sections. The main outcome is that potential temperature and salinity anomalies are highly correlated (from 0.7 to 0.9) across the lower thermocline (from 800 to 2000 dbar) in the three sections (except salinity anomalies at the Ortegale section with only  $\sim 0.6$ ), suggesting that changes may be more affected by the large scale. At deep levels below 2400 dbar, correlation of changes is also statistically significant with  $R \sim 0.7$ –0.9.

**Table 3.** *p*-Values From Durbin-Watson Test<sup>a</sup>

<i>P</i> (dbar)	Finisterre		Santander		Ortegal	
	$\Delta\theta$ (°C)	$\Delta S$	$\Delta\theta$	$\Delta S$	$\Delta\theta$	$\Delta S$
0–200	<b>0.04</b>	<b>0.00</b>	0.17	<b>0.00</b>	0.80	<b>0.07</b>
200–400	0.95	<b>0.00</b>	<b>0.00</b>	<b>0.00</b>	0.23	<b>0.01</b>
400–800	<b>0.00</b>	<b>0.02</b>	<b>0.01</b>	0.80	0.93	0.24
800–1200	<b>0.08</b>	0.12	<b>0.09</b>	<b>0.02</b>	0.62	0.12
1200–1600	<b>0.01</b>	<b>0.02</b>	<b>0.00</b>	<b>0.00</b>	0.49	0.83
1600–2000	<b>0.01</b>	<b>0.00</b>	<b>0.01</b>	<b>0.00</b>	<b>0.08</b>	0.26

<sup>a</sup>Test of autocorrelation was applied to series at isobaric levels shown in Figure 2. Zero values indicate  $p \leq 10^{-3}$ . Significant at >90% confidence level values in bold.

Finally, we focus on the correlation of the same water masses at the three sections. No significant correlation may indicate the dominance of the eddy-field, but could also indicate different regional signals of water masses variability. There are significant correlations between all three sections in the surface waters and the upper thermocline (200–400 dbar, especially in salinity, Figure 2). *R* is as high as 0.8 between Finisterre and Santander and more than 0.9 between Finisterre and Ortegal, significant at the 95% confidence level at 0–200 dbar. This correlation stands also for central waters salinity anomalies, 0.77 for Finisterre-Santander and 0.93 for Finisterre-Ortegal. For these specific layers, stats suggest large-scale influence; note that this does not contradict the dominance of mesoscale at Ortegal since the autocorrelation test shows large *p*-values except for salinity anomalies at 0–200 dbar and 200–400 dbar (Table 3).

If the time scale of the mesoscale variability is  $250 \pm 100$  days [Pingree, 1994], we might expect that 1 or 2 sections per year will undersample that temporal variability, leading to biased results. In order to get a further estimate on the uncertainty due to the low frequency sampling, we make use of the UK Met Office EN4 product [Good et al., 2013]. The product is constructed on a monthly basis as objectively analyzed fields based on observed subsurface ocean temperature and salinity, mainly from Argo float profilers within the last decade. We extracted data from the EN4 data set at grid points along 43°N, 9°W–15°W (Finisterre section) for the 2003–2013 period and computed deseasonalized time series of temperature and salinity at the same isobaric levels as our record. The approach is to compare a low-pass filtered version of the time series (representing variability at the time scale we are interested in) to a time series of the same product subsampled six-monthly (the rate of our in situ ocean time series). The standard deviation of the residuals between these two series is taken as representative of the error associated with the semiannual sampling.

The analysis was restricted to the upper 2000 dbar of the water column since there are limited data points below that level [Good et al., 2013]. Figure 4 shows monthly and 6 month averaged time series of salinity variations from the EN4 product at two representative levels (a) 200–400 dbar and (b) 1600–2000 dbar. Salinity variations observed from the sections with estimated error bars are shown for the same pressure intervals in (c) and (d), respectively. Table 5 shows a comparison between errors calculated as deviations of

**Table 4.** Correlation Coefficients (*R*) and *p*-Values for Potential Temperature and Salinity Anomalies ( $\Delta\theta$ ,  $\Delta S$ )<sup>a</sup>

Pressure Layers (dbar)	$\Delta\theta$						$\Delta S$					
	<i>R</i> <sub>Fist.</sub>	<i>p</i> <sub>Fist.</sub>	<i>R</i> <sub>Orte.</sub>	<i>p</i> <sub>Orte.</sub>	<i>R</i> <sub>Sant.</sub>	<i>p</i> <sub>Sant.</sub>	<i>R</i> <sub>Fist.</sub>	<i>p</i> <sub>Fist.</sub>	<i>R</i> <sub>Orte.</sub>	<i>p</i> <sub>Orte.</sub>	<i>R</i> <sub>Sant.</sub>	<i>p</i> <sub>Sant.</sub>
0–200 → 200–400	0.36	0.13	0.07	0.80	<b>0.66</b>	<b>0.00</b>	<b>0.69</b>	<b>0.00</b>	<b>0.66</b>	<b>0.01</b>	<b>0.79</b>	<b>0.00</b>
200–400 → 400–800	0.24	0.33	0.26	0.36	0.12	0.67	0.42	0.08	0.42	0.12	<b>0.84</b>	<b>0.00</b>
400–800 → 800–1200	0.50	0.03	0.44	0.11	0.48	0.06	<b>0.75</b>	<b>0.00</b>	<b>0.72</b>	<b>0.00</b>	–0.15	0.57
800–1200 → 1200–1600	<b>0.84</b>	<b>0.00</b>	<b>0.77</b>	<b>0.00</b>	<b>0.90</b>	<b>0.00</b>	<b>0.83</b>	<b>0.00</b>	0.56	0.03	<b>0.75</b>	<b>0.00</b>
1200–1600 → 1600–2000	<b>0.79</b>	<b>0.00</b>	<b>0.71</b>	<b>0.00</b>	<b>0.89</b>	<b>0.00</b>	<b>0.80</b>	<b>0.00</b>	<b>0.61</b>	<b>0.02</b>	<b>0.86</b>	<b>0.00</b>
1600–2000 → 2000–2400	<b>0.60</b>	<b>0.00</b>	0.59	0.02	0.45	0.08	<b>0.68</b>	<b>0.00</b>	0.35	0.21	0.33	0.22
2000–2400 → 2400–2800	0.54	0.02	<b>0.67</b>	<b>0.00</b>	<b>0.73</b>	<b>0.00</b>	0.53	0.02	<b>0.69</b>	<b>0.00</b>	<b>0.89</b>	<b>0.00</b>
2400–2800 → 2800–3200	<b>0.69</b>	<b>0.00</b>	<b>0.92</b>	<b>0.00</b>	<b>0.61</b>	<b>0.01</b>	<b>0.87</b>	<b>0.00</b>	<b>0.92</b>	<b>0.00</b>	<b>0.83</b>	<b>0.00</b>
2800–3200 → 3200–3600	<b>0.81</b>	<b>0.00</b>	<b>0.93</b>	<b>0.00</b>	<b>0.84</b>	<b>0.00</b>	<b>0.83</b>	<b>0.00</b>	<b>0.95</b>	<b>0.00</b>	<b>0.90</b>	<b>0.00</b>
3200–3600 → 3600–4000	0.44	0.10	<b>0.91</b>	<b>0.00</b>	<b>0.71</b>	<b>0.00</b>	<b>0.75</b>	<b>0.00</b>	<b>0.96</b>	<b>0.00</b>	<b>0.98</b>	<b>0.00</b>
3600–4000 → >4000	<b>0.96</b>	<b>0.00</b>	<b>0.67</b>	<b>0.01</b>	<b>0.87</b>	<b>0.00</b>	<b>0.85</b>	<b>0.00</b>	<b>0.96</b>	<b>0.00</b>	<b>0.94</b>	<b>0.00</b>

<sup>a</sup>Anomalies were averaged every 400 dbar along the Finisterre (subscript Fist.), Ortegal (Orte.), and Santander (Sant.) sections. Correlation coefficients (*R*) larger than 0.60 at >90% confidence level ( $p < 0.1$ ) are shown in bold.

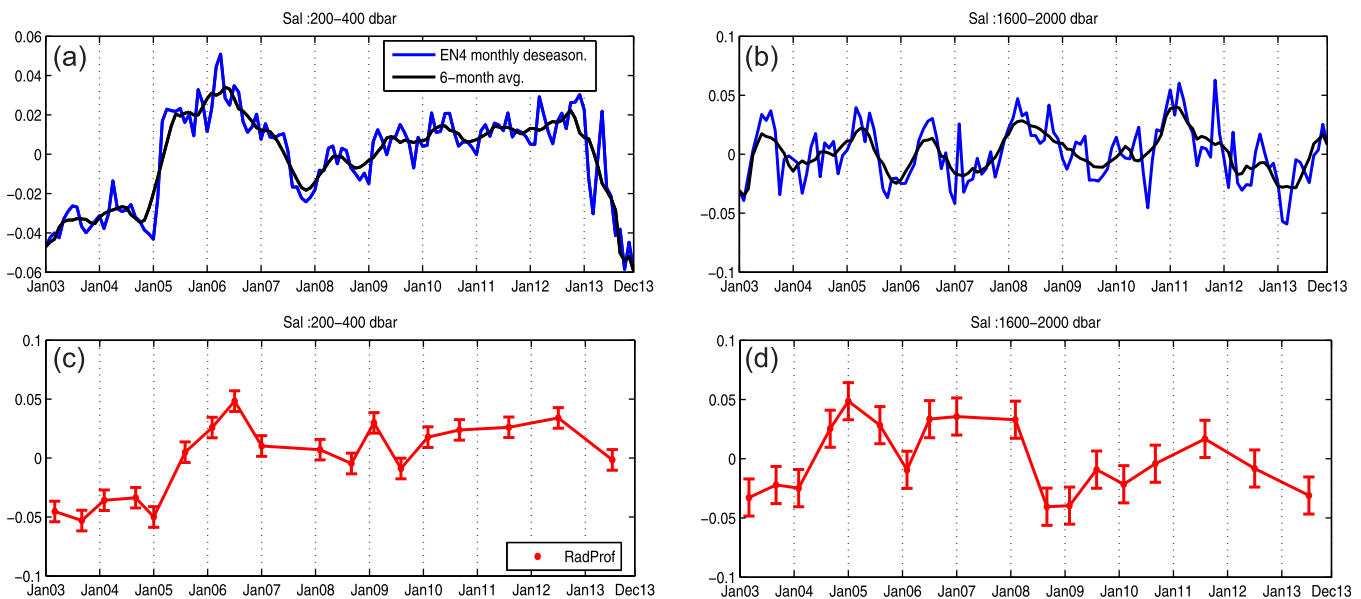


**Figure 4.** Monthly deseasonalized salinity time series from objective analysis (blue line) and 6 month moving average of time series (black line), retrieved from the EN4 UK Met Office product [Good *et al.*, 2013] for the (43°N, 9°W–15°W) region at (a) 200–400 dbar and (b) 1600–2000 dbar. Interannual variability observed along the Finisterre section (c) at the same pressure intervals and (d) with estimated error bars calculated from residuals of the blue and black lines.

the residuals of EN4 time series ( $\Delta\theta_e, \Delta S_e$ ) and the size of maximum anomalies observed in the in situ time series ( $\Delta\theta, \Delta S$ ). Estimated errors are an order of magnitude smaller than the background signal supporting also the idea that the large-scale variability has been identified above mesoscale noise.

### 5.3. Decomposition of Changes: Isopycnal Versus Heave

Having established that large-scale variations can be detected above mesoscale variability in the time series at Finisterre below the surface layer, we next examine the relative influence of heave versus isopycnal component in the observed changes. The  $\theta S$  relationship together with the average depths of isoneutrals is given in Figure 5a, vertical gradients of properties are shown as an inset (Figure 5a'), and the temporal variation of selected isoneutrals pressure  $N'$  is shown in Figure 5b. The later terms account for changes due to heave following equations (2) and (3).

Decomposition of the property changes on selected isoneutrals is shown on Figure 6. The inaccuracy of the decomposition is visible as the difference between the isobaric change versus the sum of the isopycnal and heave terms. Isopycnal changes for temperature and salinity must yield the same functional form (as constrained by density), while changes due to heave differ since they are modulated by their respective reference gradient profiles.

A dominance of isopycnal origin in the variability of central waters clearly emerges from Figure 6, particularly in the salinity record. The decade is mostly characterized by the rapid warming and salinification after the winter of 2005. Isonneutral 27.2 shoaled by about 100 m in 2005 (Figure 5b) causing immediate cooling and freshening, but after that there was a process of isopycnal warming/salinification that ended by late 2006, and the water mass has remained stable in this saltier/warmer state since then. The event in 2005 also affected the isoneutral associated with the Salinity Minimum (27.3, ~500–600 dbar). This level had a notable shift in properties after 2011 when the Salinity Minimum was up to 0.15°C warmer and 0.025 saltier than average. Changes along the isoneutrals of the upper MW to the MW core (27.5–27.7) have an almost exclusively isopycnal origin consisting of warming/salinification since

**Table 5.** Estimate of Short-Term Variability Based on the EN4 product<sup>a</sup>

$\Delta P$ (dbar)	$\Delta\theta_e$ (°C)	$\Delta\theta$ (°C)	$\Delta S_e$	$\Delta S$
0–200	0.32	1.0	0.015	0.2
200–400	0.05	0.4	0.008	1.2
400–800	0.04	0.2	0.011	0.1
800–1200	0.10	0.4	0.026	0.1
1200–1600	0.15	0.4	0.032	0.1
1600–2000	0.08	0.4	0.016	0.1

<sup>a</sup>Estimated short-term variability at the Finisterre section ( $\Delta\theta_e, \Delta S_e$ ) compared to the interannual variability exhibited by the section ( $\Delta\theta, \Delta S$ ).

of isopycnal warming/salinification that ended by late 2006, and the water mass has remained stable in this saltier/warmer state since then. The event in 2005 also affected the isoneutral associated with the Salinity Minimum (27.3, ~500–600 dbar). This level had a notable shift in properties after 2011 when the Salinity Minimum was up to 0.15°C warmer and 0.025 saltier than average. Changes along the isoneutrals of the upper MW to the MW core (27.5–27.7) have an almost exclusively isopycnal origin consisting of warming/salinification since

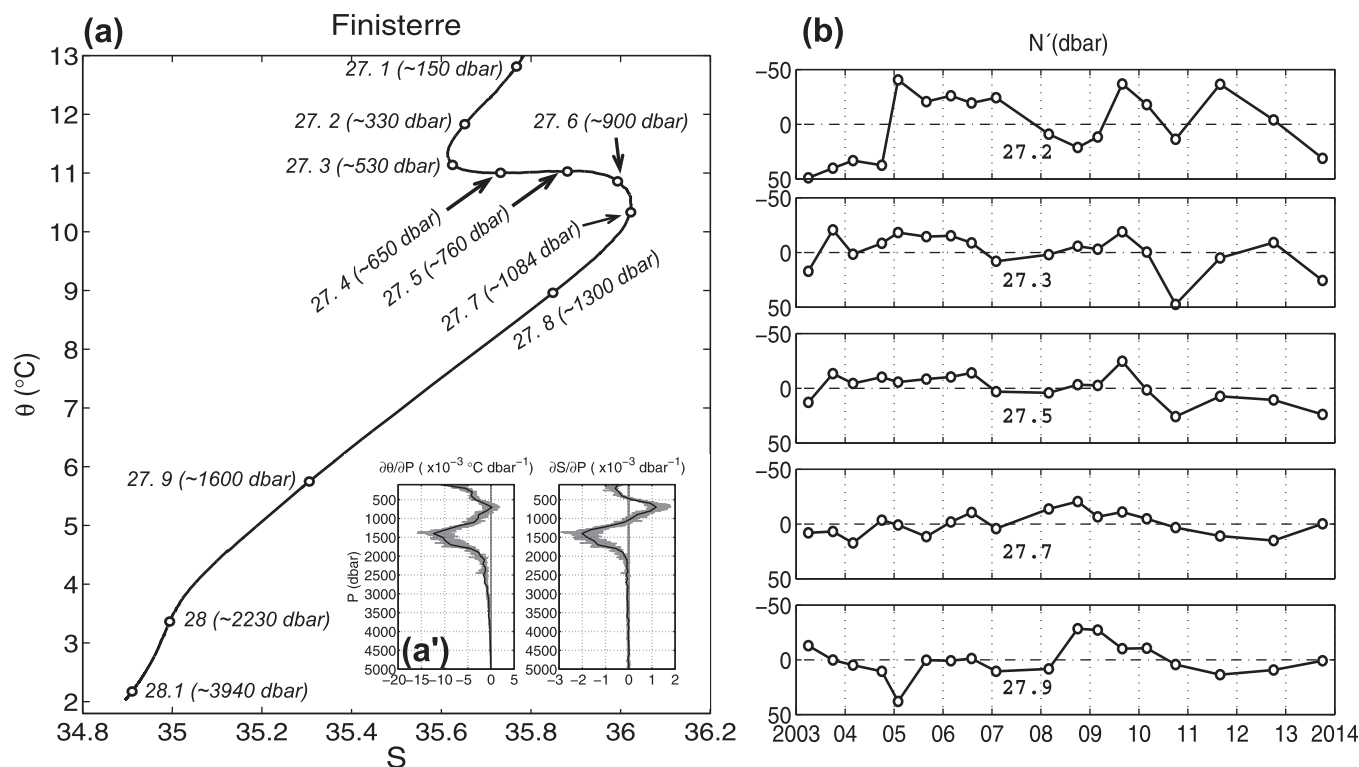


**Figure 5.** (a) Location of isoneutrals used for the study (lying at mean pressure in brackets) in the Finisterre along-section/whole time period  $\theta S$  average. (a') Potential temperature and salinity vertical gradients. Black lines represent gradient of properties averaged over time; gray lines show gradients calculated for all profiles sampled during all cruises. (b) Interannual variations of isoneutrals pressure in the 2003–2013 period.

2003 with maximum in summer 2005 followed by fresher and cooler conditions interrupted at both levels by the abrupt strong warming ( $0.3\text{--}0.4^\circ\text{C}$ ) and salinification ( $0.08\text{--}0.1$ ) of isopycnal origin in 2011. Changes on isoneutral 27.9 (LSW) show isopycnal change and heave during the sampling period. Warming/salinification by isopycnal change was observed again from 2003 to 2005, after which warming/salinification by heave was caused by the deepening of isoneutral 27.9 by about 50 dbar (see Figure 5b).

The fresher state around 2009–2011 in the deepest layer is consistent with isopycnal change; however, the weak density gradients below the permanent thermocline mean that this conclusion has low certainty. Overall, the variations in the deepest water of the Finisterre section are weak and show no clear trends.

During 2008, 2011, and 2013 there were coordinated responses across large parts of the water column so we present the vertical decomposition of changes in Figure 7. In 2008, there was cooling and freshening down to about 2500 dbar (with maximum values at  $\sim 1500$  dbar) as a combination of isopycnal change and heave. However, between the Salinity Minimum and upper MW ( $\sim 500\text{--}900$  dbar, 27.3–27.6), changes had a mainly isopycnal origin. In contrast, Figures 7b and 7e show warming and salinification across the permanent thermocline in 2011, with maximum values at  $\sim 1300$  dbar (27.8) and with an almost exclusively isopycnal origin from 500 to 2000 dbar (27.3 to  $\sim 28$ ). Changes in 2013 showed cooling and freshening of the whole water column (Figures 7c and 7f), with a maximum at 1300 dbar through a combination of isopycnal change and heave, the latter associated with the shoaling of isoneutrals 27.8 and 27.9. The water column down to the Salinity Minimum cooled by isopycnal change and warmed by heave due to the deepening of associated isoneutrals. In the next section, we will discuss changes of water mass properties in terms of the NAO-induced forcing and main North Atlantic circulation patterns affecting the Finisterre section.

## 6. Discussion

The monitoring program along the Finisterre section has provided a detailed view of interannual variability during the 2003–2013 period. The variability is the result of a complex combination of changes in large-

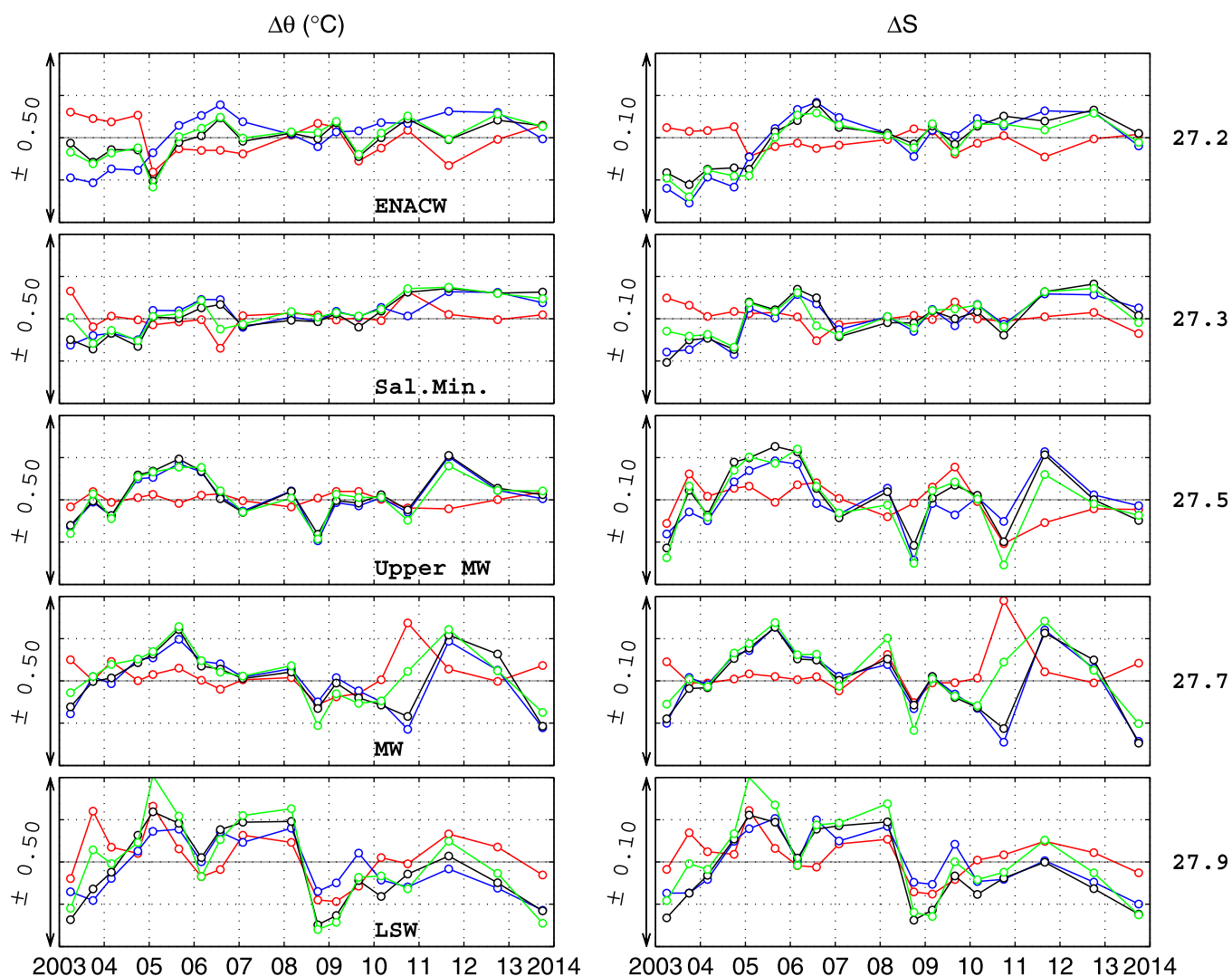


**Figure 6.** Time series of potential (left) temperature and (right) salinity decomposition of isobaric changes (black, data from section 5.1) on isopycnal change (blue) and heave (red) at selected isoneutrals: thermocline waters (ENACW, 27.2), the Salinity Minimum (27.3), Upper MW (27.5), MW core (27.7), Deep Mediterranean—LSW interface (27.9) and deep waters (ENADW, 28; LDW, 28.1). Differences between the black and green (sum of the blue and red) lines represent the inaccuracy of decomposition.

scale advective patterns, the intrinsic properties of water masses at their formation areas and local processes. The coherent response during specific years across large parts of the water column suggests an influence of the large-scale circulation pattern. In this section, we discuss the causes of the observed coherent variability in relation to the present understanding of North Atlantic circulation.

### 6.1. Climatic Indexes and Large-Scale Circulation of the North Atlantic

The North Atlantic Oscillation (NAO) is a leading pattern of weather and climate variability over the Northern Hemisphere strongly affecting the ocean through changes in heat content, gyre dynamics, and deep water formation [Hurrell and Deser, 2010]. During a negative phase of the NAO, the Labrador Current is enhanced bringing more freshwater into the subtropics, and the northward penetration of Mediterranean Water in the eastern North Atlantic also increases, there is southward displacement of the Subpolar Front in the western North Atlantic basin and the advection of more warm/salty subtropical water toward the northeastern North Atlantic [Eden and Willebrand, 2001; Núñez Riboni et al., 2012]. A high positive NAO phase is associated with the strengthening and eastward expansion of the Subpolar Gyre (SPG) bringing cooler, fresher conditions to the eastern region [Sarafanov, 2009].

Strong and rapid shifts in the winter NAO index may cause similar effects in the North Atlantic Ocean circulation as a long period of sustained NAO index [Chaudhuri et al., 2011]. For example, the circulation of the

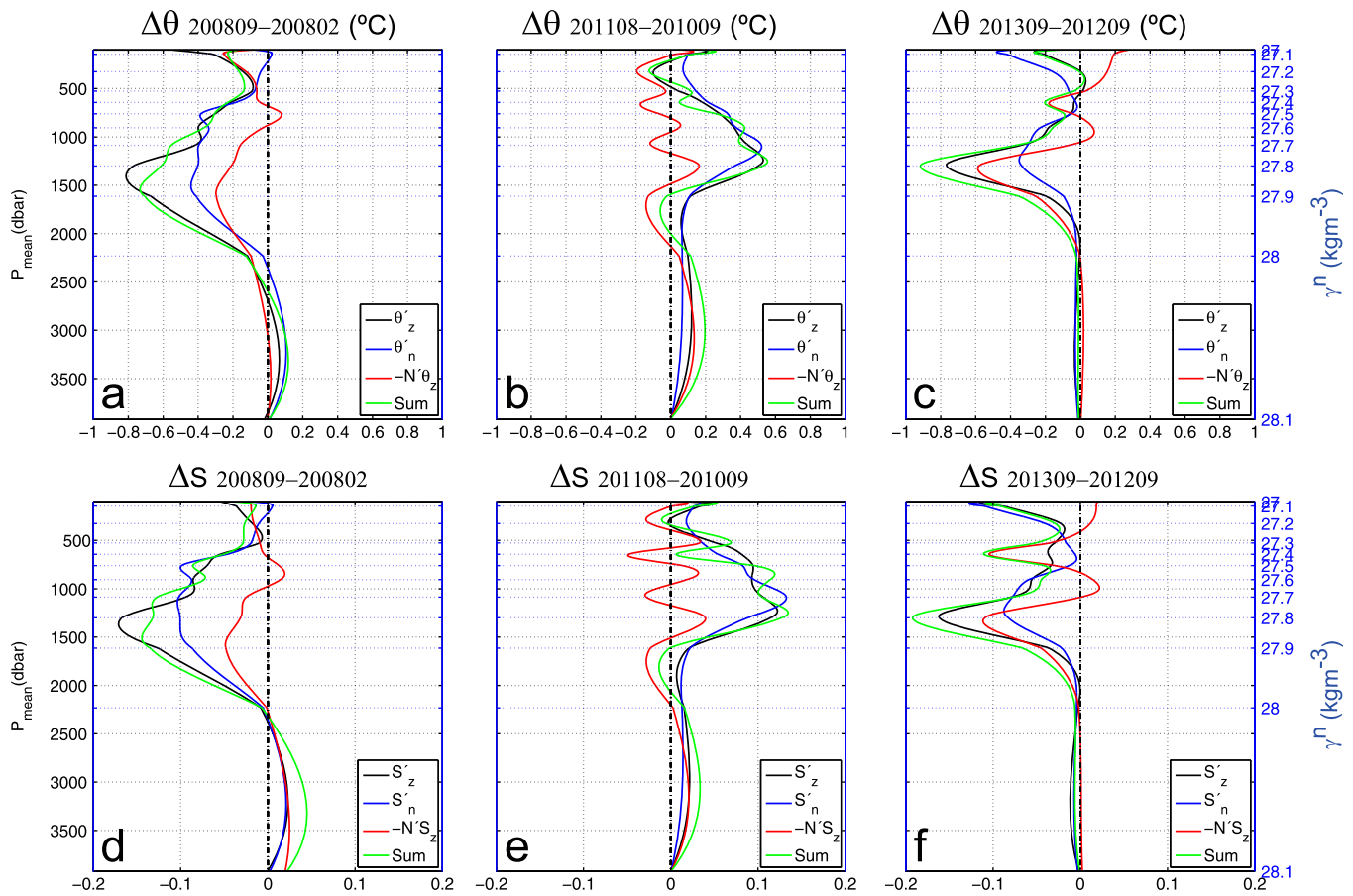


**Figure 7.** Decomposition of the (a–c) temperature and (d–f) salinity isobaric changes (black) on isopycnal changes (blue) plus changes by heave (red) following Bindoff and McDougall [1994]. The sum of both (isopycnal plus heave), shown in green, accounts for the inaccuracy of the decomposition. Method was applied to changes observed in the water column between 27 and 28.1  $\text{kgm}^{-3}$ , (left) from February 2008 to September 2008, (middle) from September 2010 to August 2011, and (right) from September 2012 to September 2013.

North Atlantic subpolar gyre appears to have weakened in response to a large shift in the NAO from a period of very high to a very low index in winter 1996 [Häkkinen and Rhines, 2004].

The data presented here indicate that the temperature and salinity in the North Atlantic eastern boundary is responsive to extreme states of the NAO. A low winter NAO index in 2010 was followed by a large increase of temperature and salinity of almost the whole water column in 2011. Years with a high positive winter NAO index, such as 2007–2008 (high positive) and 2012 (very high positive) were followed by water mass property changes of the opposite sense; cooling/freshening across much of the water column. Note that changes associated with high positive NAO events were due to heave and isopycnal change (sinking of isopycnals) while changes after the high negative NAO only involve isopycnal change (Figure 7). We do not know at this stage whether this may be a typical behavior of large negative/positive NAO years.

It has been shown that the strength and extent of the subpolar gyre can have a profound influence on the water mass properties of the subpolar gyre [Hätún et al., 2005; Häkkinen and Rhines, 2009]. An index of the strength of the gyre circulation has been developed and shown to be only indirectly related to the NAO index [Häkkinen et al., 2011a, 2011b, 2013]. The subpolar gyre index is reproduced with the NAO winter index in Figure 8 for the period 1993–2012. There is no clear relationship between the SPG index and variations in water mass properties at interannual scales in our midlatitude section. In summary, the time series presented here reflect a local oceanic response induced by the NAO. The influence is characterized by the presence of more cool/freshwater from the northwestern North Atlantic 1 year after a high positive NAO index year, and more intrusion of subtropical waters from the south 1 year after a strong negative NAO index year. The results provide more evidence of the role of the NAO in driving rapid changes in the deep ocean as well as in surface waters.

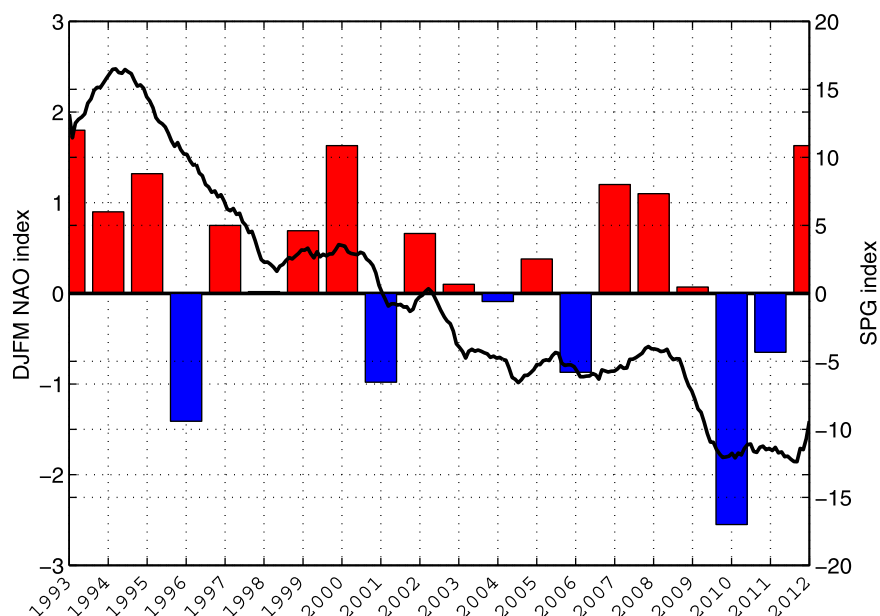


**Figure 8.** Winter (December–March) Hurrell NAO index with bars (red: positive NAO years; blue: negative NAO years), obtained as the first principal component of the winter SLP from <https://climatedataguide.ucar.edu/climate-data/hurrell-north-atlantic-oscillation-nao-index-pc-based> [NCAR Staff, 2014]. SPG index obtained as the first principal component of SSH [Häkkinen et al., 2013]

## 6.2. Changes in the Main Water Masses

Besides causing changes in advective patterns (and not unconnected with these), large-scale atmospheric variability conditions the formation of different water masses from modal to deep waters at their source areas. Next, we discuss the variability observed in each water mass.

### 6.2.1. ENACW

During the winter of 2005, the ENACW layers of the Finisterre section cooled by about  $0.5^{\circ}\text{C}$  in the upper 200 dbar and about  $0.3^{\circ}\text{C}$  in the 200–400 dbar layer. A more saline mode water was the outcome of this process, seen as isopycnal warming in the neutral levels 27.2 and 27.3, and a shoaling of isoneutral 27.2. This same pattern of change has been documented in the Bay of Biscay where it was attributed to the heat loss and the low net precipitation-minus-evaporation of the cold, dry winter affecting a wide region including the Western Mediterranean Sea [Somavilla et al., 2009]. The implication is that the winter 2005 atmospheric conditions profoundly affected a wide area of the upper ocean from the western Bay of Biscay to the eastern margin. The results are consistent with previous work that shows that the main driver for ENACW salinity variations is the local precipitation minus evaporation ( $P-E$ ) balance (directly affected by the NAO), and that properties acquired by the ENACW every winter remains at least 1 year after the water mass formation [Pérez et al., 2000]. For the deeper layers of the ENACW (the Salinity Minimum), the influences on the water mass properties are more complex because these layers can mix with warm saline Mediterranean Water and the slightly lighter Subarctic Intermediate Water (SAIW) [Pollard et al., 1996]. The results from the Finisterre section suggest that the deep ENACW was affected by the cold winter of 2005 (no change in layer thickness but significant isopycnal change), but it is possible that the conditions were also influenced by the incursion of Subarctic Intermediate Water carried by a stronger North Atlantic Current flowing north-eastward at lower depths [Häkkinen and Rhines, 2009].

### 6.2.2. MW-LSW Levels

The Finisterre section is located on the northern edge of the subtropical gyre across the theoretical pathway of MW (Figure 1). The results at MW core (800–1200 dbar) show density compensated changes consisting of warming/salinification to 2005, cooling/freshening to late 2010, and sharp changes in 2011 and 2013. We have suggested that these changes in properties, particularly after strong NAO years, may be an advective response. Note that interpreting isopycnal changes at MW levels as having advective origin may appear counter-intuitive but reflects the fact that we are dealing with a water mass characterized by large lateral

gradients. Also note that right at the core of MW there cannot be property changes by heave since the vertical gradients of temperature and salinity vanish.

These changes are consistent with the proposed response of the SPG to the NAO discussed in the literature. Periods of increasing and positive NAO index induces an expanding SPG and cooling and freshening of northern subpolar intermediate waters, but warmer and more saline MW in the eastern subtropical gyre since the spreading of the MW toward northern latitudes is blocked [Lozier and Stewart, 2008; Lozier and Sindlinger, 2009; Chaudhuri et al., 2011]. This was the case for several decades up to the mid-1990s. After the mid-1990s, the intermediate waters of northern North Atlantic warmed and became more saline as the SPG contracted and more subtropical water entered the region [Sarafanov et al., 2009]. Our results are consistent with this view, with the warming/salinification observed to 2005 being likely a response to the contracting SPG (and more spreading of MW), and the subsequent cooling and freshening possibly a response to new positive phases of the NAO (and blocking of MW).

The most significant change in the properties of the LSW was seen in autumn 2008 as a drop in temperature and salinity that lasted to 2011. A similar change was seen in the Rockall Trough (which lies to the north) in 2006–2009 and is thought to indicate the arrival of a particular vintage of LSW formed in winter 2000 [Nolan et al., 2012]. It is possible, but not certain, that the 2008 event at the Finisterre section indicates the arrival of the LSW<sub>2000</sub> there. It has long been known that the largest changes to LSW properties are those induced by changes in air-sea fluxes during winter convection at source, sometimes as a direct response to the NAO [Pickart et al., 2003; Flatau et al., 2003]. The range of property variations are so large that the variability of LSW at source may leave an imprint on the water mass far from the origin, and a range of travel times from the source to the eastern basins has been estimated based on matching Labrador Sea conditions with local changes [Read and Gould, 1992; Cunningham and Haine, 1995; Pickart et al., 2003; Yashayaev et al., 2007]. Our results suggest that such remote imprints in LSW properties may reach even further than previously assumed.

### 6.2.3. Deep Waters

The variations in the deepest water of the Finisterre section are weak and show no clear trends (see Figure 2). Though there is evidence in the literature of changes in deep waters of the North Atlantic, during the time span of our time series the deep ocean in the Atlantic Iberian basin has remained stable. Examples of observed changes include decadal density-compensated temperature anomalies formed in the subpolar gyre and then propagated equatorward [Mauritzen et al., 2012]; and rapid freshening of the deep North Atlantic over past decades [Dickson et al., 2002; Curry et al., 2003; Atkinson et al., 2012]. Atkinson et al. [2012] found a decreasing southward transport in the 3000–4700 m layer (LNADW) along 25°N, coincident with a density compensated cooling and freshening of the Denmark Strait Overflow Water in the Deep Western Boundary Current at that latitude.

## 7. Conclusions

A monitoring program of the deep ocean in the northwestern Iberia and southern Bay of Biscay, running since 2003, has provided a detailed view of interannual changes in the last decade in the midlatitude transitional intergyre region, complementing well the established monitoring programs in the subpolar and subtropical regions. The time series exhibited statistically significant autocorrelation, correlation across large portions of the water column, and geographical correlation mostly between Finisterre and Santander sections, suggesting that the sampling scheme is adequate to resolve background variability over mesoscale activity. The most comprehensive results are provided by the Finisterre section which is the deepest, longest and most often repeated. The Finisterre section has been shown to be representative of changes in the North Atlantic eastern boundary. The hydrographic time series are shown to have primarily isopycnal changes of thermohaline properties. Statistically significant trends over the time series were found in the ENACW, dominated by a change to a saltier/warmer state after the extreme winter forcing of 2005. A significant long-term trend was also observed at the transition level between MW and LSW, dominated by the change to colder/fresher conditions toward the end of the series, from 2008 to 2010. Variability below the 2000 dbar is very small, oscillating around the limits of what is measurable.

The water mass properties of the section are strongly influenced by the state of the NAO, most obviously as a rapid and local response to the high positive NAO in winters 2007–2008 and 2012 (inducing cooling and

freshening), and the extremely negative NAO index in winter 2010 (inducing warm and saline intermediate conditions). The results are consistent with present knowledge of North Atlantic circulation and its response to atmospheric circulation. The present work supports the importance of the maintenance of continuous monitoring programs of deep ocean variability, through the periodic repetition of hydrographic sections, as a valuable tool for analyzing deep ocean changes on interannual to decadal scales, including unpredictable strong shifts essential to predict future local or global climate change. The results derived from this monitoring program are expected to contribute to future revisions and further developments in long-term Spanish climate monitoring strategy.

### Acknowledgments

We thank all the technicians and the crew of R/V Cornide de Saavedra, Thalassa and Ángeles Alvariño for their support in the different occupation of the Finisterre, Ortegal and Santander sections. Data set from the series of cruises are archived at the Spanish Institute of Oceanography Data Center (<http://indamar.ieo.es/>) where they can be requested. Objective analysis fields were obtained from the UK Met Office EN4 product (<http://www.metoffice.gov.uk/hadobs/en4/>). The Hurrell North Atlantic Oscillation PC-based index was taken from the Climate Data Guide at [www.climateataguide.ucar.edu](http://www.climateataguide.ucar.edu). Sirpa Häkkinen kindly provided the Subpolar Gyre Index series. We also thank anonymous reviewers for their valuable comments. This study was performed in the frame of VACLAN (REN 2003–08193-C03-01/MAR)/COACLAN (CTM2007–64600/MAR) projects. E. Prieto is funded by a PhD grant from the Science and Innovation Department of the Spanish Government.

### References

- Atkinson, C. P., H. L. Bryden, S. A. Cunningham, and B. A. King (2012), Atlantic transport variability at 25°N in six hydrographic sections, *Ocean Sci.*, 8(4), 497–523, doi:10.5194/os-8-497-2012.
- Baker, D. J., R. W. Schmitt, and C. Wunsch (2007), Endowments and new institutions for long-term observations, *Oceanography*, 20(4), 10–14, doi:10.5670/oceanog.2007.19.
- Barnett, T. P., D. W. Pierce, K. M. AchutaRao, P. J. Gleckler, B. D. Santer, J. M. Gregory, and W. M. Washington (2005), Penetration of human-induced warming into the world's oceans, *Science*, 309(5732), 284–287, doi:10.1126/science.1112418.
- Bindoff, N. L., and T. J. McDougall (1994), Diagnosing climate change and ocean ventilation using hydrographic data, *J. Phys. Oceanogr.*, 24(6), 1137–1152, doi:10.1175/1520-0485(1994)024.
- Bretherton, F. P., R. E. Davis, and C. B. Fandry (1976), A technique for objective analysis and design of oceanographic experiments applied to MODE-73, *Deep Sea Res. Oceanogr. Abstr.*, 23, 559–582, doi:10.1016/0011-7471(76)90001-2.
- Bryden, H. L., E. L. McDonagh, and B. A. King (2003), Changes in ocean water mass properties: Oscillations or trends?, *Science*, 300(5628), 2086–2088, doi:10.1126/science.1083980.
- Chaudhuri, A. H., A. Gangopadhyay, and J. J. Bisagni (2011), Contrasting response of the Eastern and Western North Atlantic circulation to an episodic climate event, *J. Phys. Oceanogr.*, 41(9), 1630–1638, doi:10.1175/2011JPO4512.1.
- Cunningham, S. A., and T. W. N. Haine (1995), Labrador Sea water in the Eastern North Atlantic. Part II: Mixing dynamics and the advective-diffusive balance, *J. Phys. Oceanogr.*, 25(4), 666–678, doi:10.1175/1520-0485(1995)025<0666:LSWITE>2.0.CO;2.
- Cunningham, S. A., et al. (2007), Temporal variability of the Atlantic Meridional Overturning Circulation at 26.5°N, *Science*, 317(5840), 935–938, doi:10.1126/science.1141304.
- Curry, R., B. Dickson, and I. Yashayaev (2003), A change in the freshwater balance of the Atlantic Ocean over the past four decades, *Nature*, 426(6968), 826–829, doi:10.1038/nature02206.
- Dexter, P., and C. P. Summerhayes (2002), Ocean Observations—the Global Ocean Observing System (GOOS), in *Troubled Waters: Ocean Science and Governance*, edited by D. Pugh and G. Holland, chap. 11, pp. 161–178, Cambridge Univ. Press, Cambridge, U. K.
- Dickson, B., I. Yashayaev, J. Meincke, B. Turrell, S. Dye, and J. Holfort (2002), Rapid freshening of the deep North Atlantic Ocean over the past four decades, *Nature*, 416(6883), 832–837, doi:10.1038/416832a.
- Eden, C., and J. Willebrand (2001), Mechanism of interannual to decadal variability of the North Atlantic circulation, *J. Clim.*, 14(10), 2266–2280, doi:10.1175/1520-0442(2001)014<2266:MOITDV>2.0.CO;2.
- Flatau, M. K., L. Talley, and P. P. Niiler (2003), The North Atlantic oscillation, surface current velocities, and SST changes in the Subpolar North Atlantic, *J. Clim.*, 16(14), 2355–2369, doi:10.1175/2787.1.
- Frouin, R., A. F. G. Fíúza, I. Ambar, and T. J. Boyd (1990), Observations of a poleward surface current off the coasts of Portugal and Spain during winter, *J. Geophys. Res.*, 95(C1), 679–691, doi:10.1029/JC095iC01p00679.
- Good, S. A., M. J. Martin, and N. A. Rayner (2013), EN4: Quality controlled ocean temperature and salinity profiles and monthly objective analyses with uncertainty estimates, *J. Geophys. Res. Oceans*, 118, 6704–6716, doi:10.1002/2013JC009067.
- Häkkinen, S., and P. Rhines (2009), Shifting surface currents in the northern North Atlantic Ocean, *J. Geophys. Res.*, 114, C04005, doi:10.1029/2008JC004883.
- Häkkinen, S., and P. B. Rhines (2004), Decline of subpolar North Atlantic circulation during the 1990s, *Science*, 304(5670), 555–559, doi:10.1126/science.1094917.
- Häkkinen, S., P. B. Rhines, and D. L. Worthen (2011a), Warm and saline events embedded in the meridional circulation of the northern North Atlantic, *J. Geophys. Res.*, 116, C03006, doi:10.1029/2010JC006275.
- Häkkinen, S., P. B. Rhines, and D. L. Worthen (2011b), Atmospheric blocking and Atlantic multidecadal ocean variability, *Science*, 334(6056), 655–659, doi:10.1126/science.1205683.
- Häkkinen, S., P. B. Rhines, and D. L. Worthen (2013), Northern North Atlantic sea surface height and ocean heat content variability, *J. Geophys. Res. Oceans*, 118, 3670–3678, doi:10.1002/jgrc.20268.
- Hansen, J., R. Ruedy, M. Sato, and K. Lo (2010), Global surface temperature change, *Rev. Geophys.*, 48, RG4004, doi:10.1029/2010RG000345.
- Hätún, H., A. B. Sando, H. Drange, B. Hansen, and H. Valdimarsson (2005), Influence of the Atlantic subpolar gyre on the thermohaline circulation, *Science*, 309(5742), 1841–1844, doi:10.1126/science.1114777.
- Hughes, S. L., N. P. Holliday, F. Gaillard, and the ICES Working Group on Oceanic Hydrography (2012), Variability in the ICES/NAFO region between 1950 and 2009: Observations from the ICES Report on Ocean Climate, *ICES J. Mar. Sci.*, 69(5), 706–719, doi:10.1093/icesjms/fss044.
- Hurrell, J., and NCAR Staff (2014), The Climate Data Guide: Hurrell North Atlantic Oscillation (NAO) Index (PC-Based). [Available at <https://climateataguide.ucar.edu/climate-data/hurrell-north-atlantic-oscillation-nao-index-pc-based/>]
- Hurrell, J. W., and C. Deser (2010), North Atlantic climate variability: The role of the North Atlantic Oscillation, *J. Mar. Syst.*, 79(3–4), 231–244, doi:10.1016/j.jmarsys.2008.11.026.
- Iorga, M. C., and M. S. Lozier (1999), Signatures of the Mediterranean outflow from a North Atlantic climatology: 2. Diagnostic velocity fields, *J. Geophys. Res.*, 104(C11), 26,011–26,029, doi:10.1029/1999JC900204.
- Jackett, D. R., and T. J. McDougall (1997), A neutral density variable for the World's Oceans, *J. Phys. Oceanogr.*, 27(2), 237–263, doi:10.1175/1520-0485(1997)027<0237:ANDVFT>2.0.CO;2.
- Joyce, T., C. Corry, and M. Stalcup (1994), WOCE operations manual, vol. 3, The Observational Programme, WOCE Report No. 68/91, Woods Hole, Mass.

- Latif, M., and T. P. Barnett (1996), Decadal climate variability over the North Pacific and North America: Dynamics and predictability, *J. Clim.*, *9*(10), 2407–2423, doi:10.1175/1520-0442(1996)009<2407:DCVOTN>2.0.CO;2.
- Lindstrom, E., et al. (2012), A framework for ocean observing. By the task team for an Integrated Framework for Sustained Ocean Observing, *IOC/INF-1284*, UNESCO, doi:10.5270/OceanObs09-FOO.
- Lozier, M. S., and L. Sindlinger (2009), On the source of Mediterranean overflow water property changes, *J. Phys. Oceanogr.*, *39*(8), 1800–1817, doi:10.1175/2009JPO4109.1.
- Lozier, M. S., and N. M. Stewart (2008), On the temporally varying northward penetration of Mediterranean overflow water and eastward penetration of Labrador Sea Water, *J. Phys. Oceanogr.*, *38*(9), 2097–2103, doi:10.1175/2008JPO3908.1.
- Mauritzen, C., A. Melsom, and R. Sutton (2012), Importance of density-compensated temperature change for deep North Atlantic Ocean heat uptake, *Nat. Geosci.*, *5*(12), 905–910, doi:10.1038/ngeo1639.
- Mazé, J. P., M. Arhan, and H. Mercier (1997), Volume budget of the eastern boundary layer off the Iberian Peninsula, *Deep Sea Res. Part I*, *44*(9–10), 1543–1574, doi:10.1016/S0967-0637(97)00038-1.
- Memery, L., G. Reverdin, J. Paillet, and A. Oschlies (2005), Introduction to the POMME special section: Thermocline ventilation and biogeochemical tracer distribution in the northeast Atlantic Ocean and impact of mesoscale dynamics, *J. Geophys. Res.*, *110*, C07S01, doi:10.1029/2005JC002976.
- Nolan, G., K. Lyons, S. Fennell, G. Westbrook, T. M. Grath, and A. Berry (2012), Annex 9: Regional report—Ireland area (area 4b), in *ICES 2012 Report of the Working Group on Oceanic Hydrography (WGOH)*, *CM 2012/SSGEF:03*, pp. 59–68, ICES Headquarters, Copenhagen.
- Núñez Riboni, I., M. Bersch, H. Haak, J. H. Jungclauss, and K. Lohmann (2012), A multi-decadal meridional displacement of the Subpolar Front in the Newfoundland basin, *Ocean Sci.*, *8*(1), 91–102, doi:10.5194/os-8-91-2012.
- Paillet, J., and H. Mercier (1997), An inverse model of the eastern North Atlantic general circulation and thermocline ventilation, *Deep Sea Res., Part I*, *44*(8), 1293–1328, doi:10.1016/S0967-0637(97)00019-8.
- Peliz, A., J. Dubert, A. M. P. Santos, P. B. Oliveira, and B. Le Cann (2005), Winter upper ocean circulation in the western Iberian basin—Fronts, eddies and poleward flows: An overview, *Deep Sea Res., Part I*, *52*(4), 621–646, doi:10.1016/j.dsr.2004.11.005.
- Pérez, F. F., R. T. Pollard, J. F. Read, V. Valencia, J. M. Cabanas, and A. F. Ríos (2000), Climatological coupling of the thermohaline decadal changes in central water of the eastern North Atlantic, *Sci. Mar.*, *64*(3), 347–353, doi:10.3989/scimar.2000.64n3347.
- Pickart, R. S., F. Straneo, and G. W. K. Moore (2003), Is Labrador Sea Water formed in the Irminger basin?, *Deep Sea Res., Part I*, *50*(1), 23–52, doi:10.1016/S0967-0637(02)00134-6.
- Pingree, R. D. (1973), A component of Labrador Sea Water in the Bay of Biscay, *Limnol. Oceanogr.*, *18*(5), 711–718, doi:10.4319/lo.1973.18.5.0711.
- Pingree, R. D. (1994), Winter warming in the southern Bay of Biscay and Lagrangian eddy kinematics from a deep-drogued Argos buoy, *J. Mar. Biol. Assoc. U. K.*, *74*(1), 107–128, doi:10.1017/S0025315400035700.
- Pingree, R. D., and B. Le Cann (1992a), Anticyclonic eddy X91 in the southern Bay of Biscay, May 1991 to February 1992, *J. Geophys. Res.*, *97*(C9), 14,353–14,367.
- Pingree, R. D., and B. Le Cann (1992b), Three anticyclonic slope water oceanic eddies (SWODDIES) in the Southern Bay of Biscay in 1990, *Deep Sea Res., Part A*, *39*(7–8), 1147–1175, doi:10.1016/0198-0149(92)90062-X.
- Pollard, R. T., and S. Pu (1985), Structure and circulation of the upper Atlantic Ocean northeast of the Azores, *Prog. Oceanogr.*, *14*(1–4), 443–462, doi:10.1016/0079-6611(85)90022-9.
- Pollard, R. T., M. J. Griffiths, S. A. Cunningham, J. F. Read, F. F. Pérez, and A. F. Ríos (1996), Vivaldi 1991—A study of the formation, circulation and ventilation of Eastern North Atlantic Central Water, *Prog. Oceanogr.*, *37*(2), 167–192, doi:10.1016/S0079-6611(96)00008-0.
- Polyakov, I., V. Alexeev, U. Bhatt, E. Polyakova, and X. Zhang (2010), North Atlantic warming: Patterns of long-term trend and multidecadal variability, *Clim. Dyn.*, *34*, 439–457, doi:10.1007/s00382-008-0522-3.
- Prieto, E., C. González-Pola, A. Lavín, R. F. Sánchez, and M. Ruiz-Villarreal (2013), Seasonality of intermediate waters hydrography west of the Iberian Peninsula from an 8 yr semiannual time series of an oceanographic section, *Ocean Sci.*, *9*(2), 411–429, doi:10.5194/os-9-411-2013.
- Read, J. F., and W. J. Gould (1992), Cooling and freshening of the subpolar North Atlantic Ocean since the 1960s, *Nature*, *360*(6399), 55–57, doi:10.1038/360055a0.
- Richardson, P. L., A. S. Bower, and W. Zenk (2000), A census of meddies tracked by floats, *Prog. Oceanogr.*, *45*(2), 209–250, doi:10.1016/S0079-6611(99)00053-1.
- Sarafanov, A. (2009), On the effect of the North Atlantic Oscillation on temperature and salinity of the subpolar North Atlantic intermediate and deep waters, *ICES J. Mar. Sci.*, *66*(7), 1448–1454, doi:10.1093/icesjms/fsp094.
- Sarafanov, A., H. Mercier, A. Falina, A. Sokov, and P. Lherminier (2010), Cessation and partial reversal of deep water freshening in the northern North Atlantic: Observation-based estimates and attribution, *Tellus, Ser. A*, *62*(1), 80–90, doi:10.1111/j.1600-0870.2009.00418.x.
- Sarafanov, A. A., A. V. Sokov, and A. S. Falina (2009), Warming and salinification of Labrador Sea Water and deep waters in the subpolar North Atlantic at 60°N in 1997–2006, *Oceanology*, *49*, 193–204, doi:10.1134/S0001437009020040.
- Somavilla, R., C. Gonzalez-Pola, C. Rodriguez, S. A. Josey, R. F. Sanchez, and A. Lavín (2009), Large changes in the hydrographic structure of the Bay of Biscay after the extreme mixing of winter 2005, *J. Geophys. Res.*, *114*, C01001, doi:10.1029/2008JC004974.
- van Aken, H. M. (2000a), The hydrography of the mid-latitude Northeast Atlantic Ocean. I: The deep water masses, *Deep Sea Res., Part I*, *47*(5), 757–788, doi:10.1016/S0967-0637(99)00092-8.
- van Aken, H. M. (2000b), The hydrography of the mid-latitude Northeast Atlantic Ocean. II: The intermediate water masses, *Deep Sea Res., Part I*, *47*(5), 789–824, doi:10.1016/S0967-0637(99)00112-0.
- van Aken, H. M. (2001), The hydrography of the mid-latitude Northeast Atlantic Ocean—Part III: The subducted thermocline water mass, *Deep Sea Res., Part I*, *48*(1), 237–267, doi:10.1016/S0967-0637(00)00059-5.
- van Aken, H. M., M. F. de Jong, and I. Yashayaev (2011), Decadal and multi-decadal variability of Labrador Sea Water in the north-western North Atlantic Ocean derived from tracer distributions: Heat budget, ventilation, and advection, *Deep Sea Res., Part I*, *58*(5), 505–523, doi:10.1016/j.dsr.2011.02.008.
- von Storch, H., and F. Zwiers (2001), *Statistical Analysis in Climate Research*, Cambridge Univ. Press, Cambridge, U. K.
- Wunsch, C. (1999), The interpretation of short climate records, with comments on the North Atlantic and Southern Oscillations, *Bull. Am. Meteorol. Soc.*, *80*(2), 245–255, doi:10.1175/1520-0477(1999)080<0245:TIOSCR>2.0.CO;2.
- Yashayaev, I., M. Bersch, and H. M. van Aken (2007), Spreading of the Labrador Sea Water to the Irminger and Iceland basins, *Geophys. Res. Lett.*, *34*, L10602, doi:10.1029/2006GL028999.